scientific reports

Check for updates

OPEN

Periodontitis promotes hepatocellular carcinoma in Stelic Animal model (STAM) mice

Tasuku Ohno[1], Takeshi Kikuchi[1]✉, Yuki Suzuki[1], Ryoma Goto[1], Daiki Takeuchi[1], Jun-ichiro Hayashi[1], Eisaku Nishida[1], Genta Yamamoto[1], Shun Kondo[1], Kouta Ono[1], Shuji Nomoto[2] & Akio Mitani[1]

Periodontitis is a prevalent oral inflammatory disease that leads to alveolar bone loss and may exert an adverse impact on systemic health. Periodontal disease may be associated with hepatocellular carcinoma (HCC); however, the mechanism of such an association is unknown. In this study, Stelic Animal model (STAM) mice, a model of nonalcoholic steatohepatitis (NASH)-HCC, were induced to develop periodontitis and subjected to histopathological and immunological analyses. HCC progression was greater in STAM mice with experimental periodontitis compared with that in STAM mice without experimental periodontitis. Tumor necrosis factor-α (TNFα), matrix metalloproteinase-9 (MMP9), collagen 1, and angiopoietin-like protein 2 (ANGPTL2) gene expression was significantly increased in the liver of the periodontitis group. ANGPTL2 was previously reported to be involved in the pathogenesis of periodontitis, and HCC and ANGPTL2 protein tended to be more abundant in the pocket epithelium of STAM mice with experimental periodontitis than in control STAM mice. ANGPTL2 levels in the serum of STAM mice with experimental periodontitis tended to be higher than in control STAM mice. Our results indicate that ANGPTL2 is produced in chronically inflamed periodontal tissue and then travels to the liver via the bloodstream where it accumulates to promote the progression of hepatocellular carcinoma.

Keywords Experimental periodontitis, Hepatocellular carcinoma, Angiopoietin-like protein, STAM mouse

Periodontal disease is a chronic inflammatory disease in which a bacterial biofilm causes periodontal tissue destruction[1]. It often causes systemic deterioration by the induction of inflammatory factors, such as inflammatory cytokines (IL1β, IL6, and TNFα) in periodontal tissue component cells and immune cells upon bacterial stimulation. This immune response causes systemic effects via the bloodstream[2,3]. Several studies have reported the relationship between periodontal disease and liver disease. For example, translocation of *Porphyromonas gingivalis*, an important periodontal pathogen, from the oral cavity to the liver may affect the pathogenesis of diabetes by influencing hepatic glycogenesis[4]. In addition, dental *P. gingivalis* infection may be important in nonalcoholic steatohepatitis (NASH) progression via upregulation of the Toll-like receptor 2 signaling pathway and activation of inflammasomes[5]. Moreover, experimental periodontitis significantly upregulates serum IL6 and SAA gene expression in the liver[6]. A recent epidemiological study showed that periodontal disease exacerbated the pathology of hepatocellular carcinoma (HCC)[7]. HCC is the most common type of liver cancer, accounting for 85–90% of all primary liver cancers. It is also one of the most lethal, having a significant impact worldwide[8]. HCC often develops subsequent to viral infections, such as hepatitis B and C, chronic hepatitis caused by alcoholism, and cirrhosis. Recently, the rate of HCC developing from NASH has been increasing, and early prevention of liver cancer caused by NASH is important. Although the link between NASH and periodontal disease is becoming clearer, no reports on the detailed mechanisms linking periodontal disease and HCC have been published.

Angiopoietins (angiopoietin 1–4) are secreted proteins with an N-terminal coiled-coil domain and a C-terminal fibrinogen-like domain that have important functions in angiogenesis and stem cell maintenance. Eight molecules have been identified that structurally resemble Angiopoietin but cannot bind to Tie2, a specific receptor for Angiopoietin, or its family member Tie1, and were named angiopoietin-like proteins (ANGPTLs)[9,10]. Excess activity of one ANGPTL, ANGTPL2, is closely related to the pathogenesis of diabetes, metabolic diseases, and various cancers by causing chronic inflammation[11,12]. Specifically, ANGPTL2 promotes tumor metastasis

[1]Department of Periodontology, School of Dentistry, Aichi Gakuin University, 2-11 Suemoridori, Chikusa-ku, Nagoya, Aichi 464–8651, Japan. [2]Department of Surgery, School of Dentistry, Aichi Gakuin University, Nagoya, Japan. ✉email: tkikuchi@dpc.agu.ac.jp

in HCC[13]. Previously, we demonstrated that ANGPTL2 levels are significantly increased in gingival crevicular fluid collected from patients with periodontitis[14].

We hypothesized that ANGPTL2 mediates periodontal disease and tumor metastasis in HCC. Therefore, we induced experimental periodontitis in NASH-HCC model mice and examined the pathological progression of HCC.

Materials and methods

Animal studies

Stelic Animal model (STAM) mice were used as a NASH-HCC model and established as described previously[15]. A periodontitis mouse model (Fig. 1A) was established as previously described[16]. Eleven-week-old male STAM mice were obtained from SMC Laboratory (Tokyo, Japan) and 11-week-old male C57BL/6 mice were obtained from Chube Kagakushizai (Nagoya, Japan). These mice were housed in a specific pathogen-free animal facility in individual cages (184 × 332 × 147 mm, 3 mice per cage) at 24 ± 1.0 °C under a 12 h light/dark cycle. STAM mice were fed a high-fat diet and C57BL/6 mice were fed a standard diet and both strains had access to water ad libitum. In the experimental periodontitis experiment, mice were divided into three groups: normal (n = 6), STAM (n = 6), and STAM with experimental periodontitis (n = 6). When STAM mice reached 12 weeks of age, a nylon suture was ligated around the cervical portion of the maxillary second molar (M2) to induce experimental periodontitis. Before treatment, mice were anesthetized with a mixture of three different anesthetics, medetomidine hydrochloride, midazolam, and butorphanol tartrate, and efforts were made to minimize suffering. Mice that maintained the ligation for the duration of the experiment period were included in the final analysis. Mice in which the suture ligated to the teeth detached or that died during the experiment were excluded. Four weeks after ligation, mice in the three groups were scheduled for euthanasia; however, six STAM mice died before this time. Overall, we used 18 STAM mice and 6 C57BL/6 mice. For experiments involving recombinant ANGPTL2 (rANGPTL2; R&D systems, Minneapolis, MN, USA) administration, mice were divided into two groups: STAM (n = 6) and STAM with intraperitoneal administration of ANGPTL2 (n = 6). In the latter group, rANGPTL2 was intraperitoneally administered at 10 ng/g using a 30G needle. The volume of fluid administered per individual was calculated based on body weight on the day of administration (unit: 0.01 mL). The sham group was treated with PBS. Dosing was scheduled once every 2 weeks (total of two doses at 12 and 14 weeks of age). The primary outcomes were inflammatory cell infiltration of gingiva, alveolar bone resorption, HCC progression, and expression of genes encoding inflammatory cytokines, ANGPTLs and MMPs in the liver, and ANGPTLs in serum. Sample size was calculated using G*power 3.1[17]. All procedures were approved by Aichi Gakuin Animal Research Committee (No. AGUD466-1). All animal experiments were conducted in accordance with national guidelines

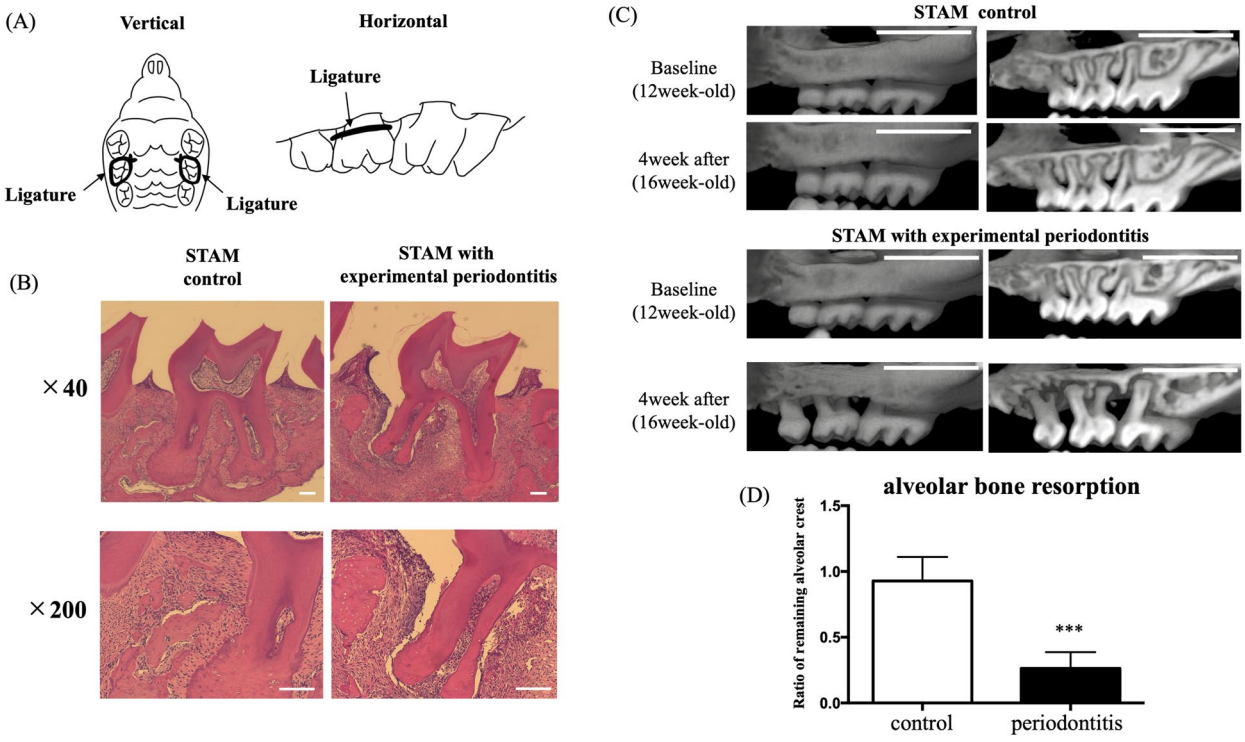

Figure 1. Induction of periodontitis in STAM mice. (**A**) Scheme of the ligature around the cervical portion of M2 (both sides). (**B**) Hematoxylin & eosin-stained gingival tissue on the mesial side of M2. Scale bar: 100 µm. (**C**) Comparison of mandibles from STAM mice with and without periodontitis using micro-CT. Micro-CT images of mandibles are shown. Scale bar: 1000 µm. (**D**) The ratio of the remaining alveolar crest bone to the root length ($n = 6$). Differences among groups were analyzed using Student's t-test. Data are expressed as the mean ± SD. $^{***}p < 0.001$.

and the relevant laws regarding the protection of animals. All animal studies were performed in compliance with the ARRIVE (Animal Research: Reporting of In Vivo Experiments) 2.0 guidelines. Animals have been euthanized by cervical dislocation after CO_2 inhalation following AVMA Guidelines for the Euthanasia of Animals: 2020 Edition (American Veterinary Medical Association). Samples were collected after slaughter.

Histological analysis and immunohistochemistry

Four weeks after ligation, maxillae were processed for hematoxylin and eosin (H&E) staining and immunohistochemistry. Maxillae were demineralized in 10% EDTA for 7 days at 4 °C, paraffin embedded, and sectioned at 4-μm thickness. First, each section was stained with H&E for histological observation. Immunohistochemistry for ANGPTL2 (Proteintech Group, Chicago, IL, USA) was then carried out. The liver was fixed in 10% formalin for 24 h and embedded in paraffin. Tissue sections (2 μm) were prepared, stained with H&E, and observed under a microscope (Keyence Japan, Osaka, Japan). The number of ANGPTL2-positive cells in six defined areas (1×10^4 μm^2 per area at 200× magnification) were counted on each slide by two independent blinded investigators. Cells in periodontal tissue with stained cytoplasm and no stained nuclei were counted as positive cells.

Quantification of alveolar bone resorption

Absorption of alveolar bone was assessed as described previously using a Rigaku R mCT scanning device (Rigaku, Tokyo, Japan) at 12 and 16 weeks of age[18]. The data were analyzed using Tri/3D-BON (Ratoc Systems, Osaka, Japan). Bone resorption was blindly calculated by two skilled investigators as the distance from the cementoenamel junction to the alveolar crest. Detailed measurement methods are described in Supplemental Appendix (Appendix Fig. 1).

Real-time polymerase chain reaction analysis

Quantitative PCR analyses using TaqMan Universal PCR master mix and TaqMan gene expression assays (Applied Biosystems, Foster City, CA, USA) were performed to quantify mRNA levels. The TaqMan gene expression assays used were for mouse *IL1B* (Mm00434228_m1), *IL6* (Mm00446190_m1), *TNFα* (Mm00443258_m1), *ANGPTL2* (Mm00507897_m1), *ANGPTL4* (Mm00480431_m1), *MMP2* (Mm00439498_m1), *MMP9* (Mm00442991_m1), and *Col1* (Mm00483888_m1) (all Thermo Fischer Scientific, Wilmington, DE, USA). All mRNA levels were normalized to β-actin (Mm02619580_g1, Thermo Fischer Scientific). Quantitative PCR was performed using the StepOnePlus Real-Time System, following the manufacturer's instructions (Thermo Fisher Scientific). The relative change in gene expression was calculated using the $2^{-\Delta\Delta Ct}$ method.

Western blotting

Western blotting was performed as previously described[14]. Liver tissues were lysed using CelLytic M lysis buffer (Sigma-Aldrich, St. Louis, MO, USA) with a protease inhibitor cocktail (Nacalai Tesque, Kyoto, Japan) and phosphatase inhibitor cocktail (Nacalai Tesque). Proteins were separated by SDS-PAGE (Bio-Rad Laboratories, Hercules, CA, USA) and transferred to polyvinylidene fluoride membranes (Bio-Rad Laboratories). Rabbit anti-mouse ANGPTL2 polyclonal antibody (Proteintech Group) and rabbit anti-mouse β-actin monoclonal antibody (Cell Signaling Technologies, Beverly, MA, USA) were used as primary antibodies. A goat anti-rabbit IgG (Cell Signaling Technologies) secondary antibody was used to detect ANGPTL2 and β-actin.

Enzyme-linked immunosorbent assay (ELISA)

ANGPTL2 protein in peripheral blood was determined using an ANGPTL2 ELISA kit (Elabscience Biotechnology, Houston, TX, USA). Blood was collected from the aorta of control mice, STAM mice, and STAM mice with periodontitis at 16 weeks of age.

Statistical analysis

Statistical analyses were performed using PASW Statistics software (version 18.0; SPSS Japan, Tokyo, Japan). Differences among groups were calculated using one-factor analysis of variance (ANOVA). Student's *t*-test was also applied for comparisons between two groups. Data are expressed as the mean ± standard deviation (SD). Statistical significance was determined at $p < 0.05$. 95% confidence intervals were also calculated with the PASW statistics software.

Results

Inflammatory cell infiltration and alveolar bone resorption induced by experimental periodontitis in STAM mice

Histological evaluation of ligatured STAM mice showed characteristic periodontitis with inflammatory cell infiltration in the epithelium and connective tissue around the second molars (Fig. 1B). The ligature also caused destruction of alveolar bone, and the alveolar bone surfaces of ligatured STAM mice showed an irregular shape and bone resorption was observed mainly in the interdental area around the second molar (Fig. 1C). The degree of alveolar bone resorption in ligatured STAM mice was significantly greater than that in STAM mice without ligature placement (Fig. 1D).

Experimental periodontitis promotes HCC progression in STAM mice

Sixteen-week-old STAM mice showed greater progression of HCC than control mice (Fig. 2A,B), while 16-week-old STAM mice with experimental periodontitis showed more pronounced progression of HCC than 16-week-old STAM mice without experimental periodontitis (Fig. 2C). H&E staining showed that 16-week-old STAM mice

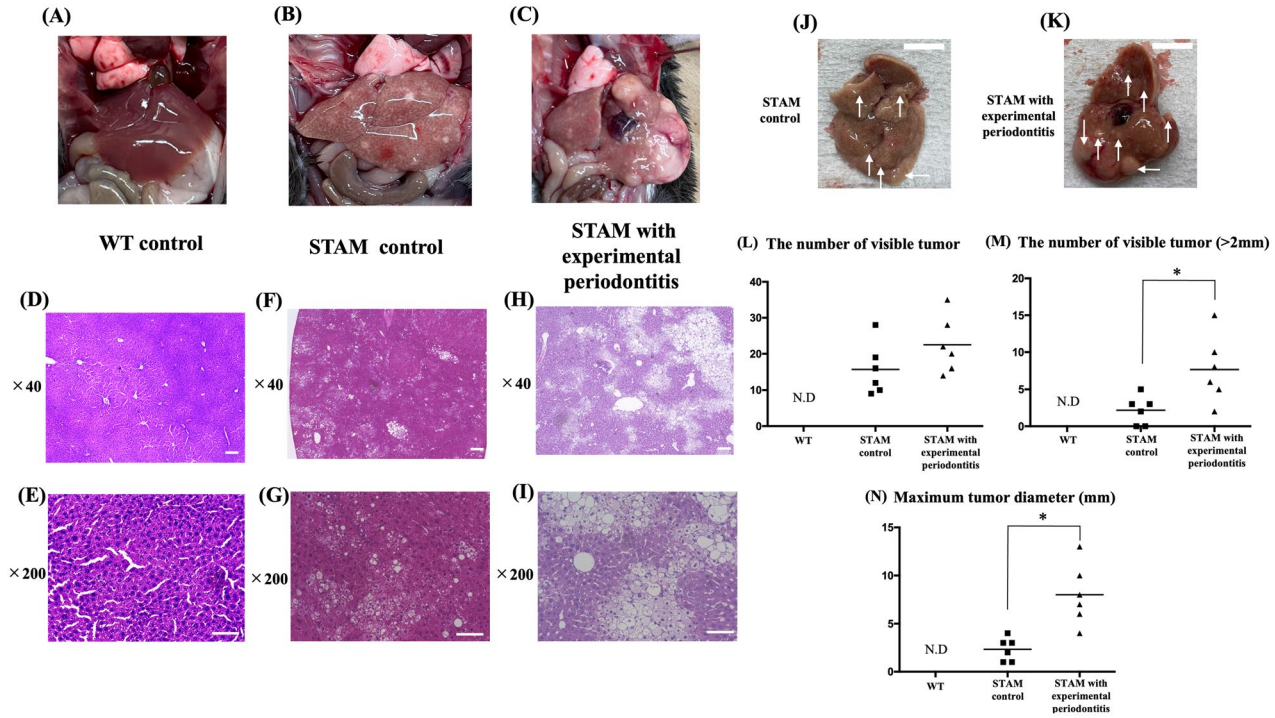

Figure 2. Macroscopic, histological features of STAM mice with experimental periodontitis. (**A**–**C**) Representative macroscopic appearance of livers from wild-type (C57BL/6), STAM, and periodontitis-induced STAM mice at 16 weeks old. (**D**–**I**) H&E-stained liver sections from wild-type, STAM, and periodontitis-induced STAM mice at 16 weeks old. Scale bar: 100 μm, magnification ×40, ×200. (**J**, **K**) The liver of STAM mice showed a granular surface and tumor protrusion. Arrowheads indicate HCCs. (**L**–**N**) Tumor characteristics of STAM mice with experimental periodontitis. Visible tumor counts are shown in (**L**). The number of visible tumors larger than 2 mm (**M**) and maximum tumor diameter (**N**) were determined. Differences among groups were analyzed using one-way ANOVA. Data are expressed as the mean ± SD ($n = 6$). *$p < 0.05$. N.D: not detected.

with experimental periodontitis had more severe vacuolar degeneration in the liver than 16-week-old STAM mice without experimental periodontitis (Fig. 2D–I) Furthermore, Sixteen-week-old STAM mice with experimental periodontitis showed a trend toward a greater number of visible tumors, a significant increase in the mean number of visible tumors larger than 2 mm, and a significant increase in the mean value of maximum tumor diameter compared with 16-week-old STAM mice without experimental periodontitis (Fig. 2J–N). In contrast, no differences were observed between the two groups regarding body weight or liver weight (Appendix Fig. 2).

Induction of experimental periodontitis in STAM mice increases expression of genes encoding inflammatory cytokines and digestive enzymes in the liver

We investigated eight genes in this study. First, TNFα, IL6 and IL1β were assessed to investigate the state of inflammation in liver cancer. TNFα gene expression in the liver was significantly higher in STAM mice with experimental periodontitis compared with that of STAM mice without periodontitis (Fig. 3A). IL6 gene expression tended to be higher in STAM mice with experimental periodontitis than in STAM mice without periodontitis (Fig. 3B), while IL1β gene expression did not differ between these groups (Fig. 3C). Second, Collagen 1, MMP2 and MMP9 were assessed to investigate the potential of cancer cell invasion and migration. Collagen 1 gene expression in liver was significantly higher in STAM mice with experimental periodontitis than in STAM mice without periodontitis (Fig. 3D). MMP9 gene expression was significantly higher in STAM mice with experimental periodontitis than in STAM mice without periodontitis (Fig. 3E). MMP2 gene expression was increased in STAM mice with experimental periodontitis compared with that in STAM mice without periodontitis, albeit not significantly (Fig. 3F). Third, ANGPTL2 and ANGPTL4 were assessed because these factors are associated with periodontal disease and various cancers. The expression levels of ANGPTL2 and ANGPTL4 genes were significantly higher in STAM mice with experimental periodontitis than in STAM mice without periodontitis (Fig. 3G, H).

ANGPTL2 expression in gingiva and liver of STAM mice is markedly increased by induction of experimental periodontitis

ANGPTL2-positive cells in periodontal tissue were significantly higher in STAM mice with experimental periodontitis than in wild-type mice and STAM mice without periodontitis (Fig. 4A–D). ANGPTL2 levels in the serum of STAM mice with experimental periodontitis tended to be higher than in STAM mice without periodontitis (Fig. 4E). ANGPTL2 protein production in the liver was also significantly higher in STAM mice with experimental periodontitis than in STAM mice without periodontitis (Fig. 4F, G).

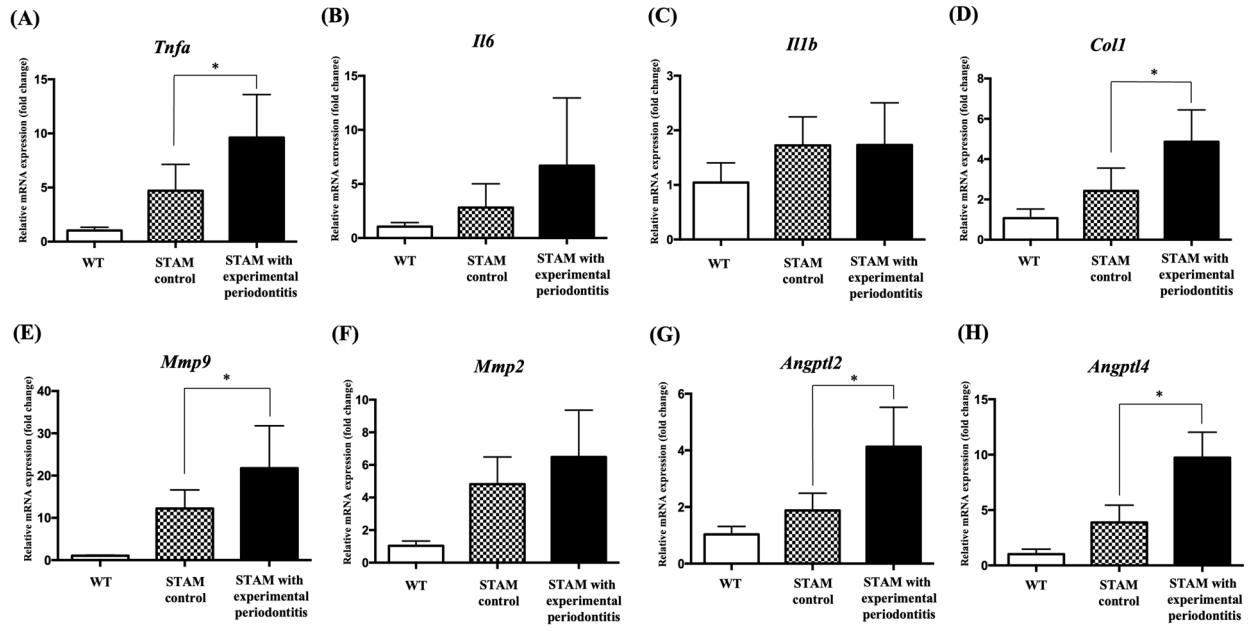

Figure 3. Gene expression in the liver of wild-type mice, STAM mice, and STAM mice with experimental periodontitis. Levels of inflammatory cytokines (**A**–**C**), collagen type 1 (Col1) (**D**), MMP9 and 2 (**E**, **F**), and ANGTPL2 and 4 (**G**, **H**) mRNA in the liver of STAM mice with experimental periodontitis were compared with those of STAM mice without experimental periodontitis and normal mice. Differences among groups were analyzed using one-way ANOVA. Data are expressed as the mean ± SD ($n = 6$). $^{*}p < 0.05$.

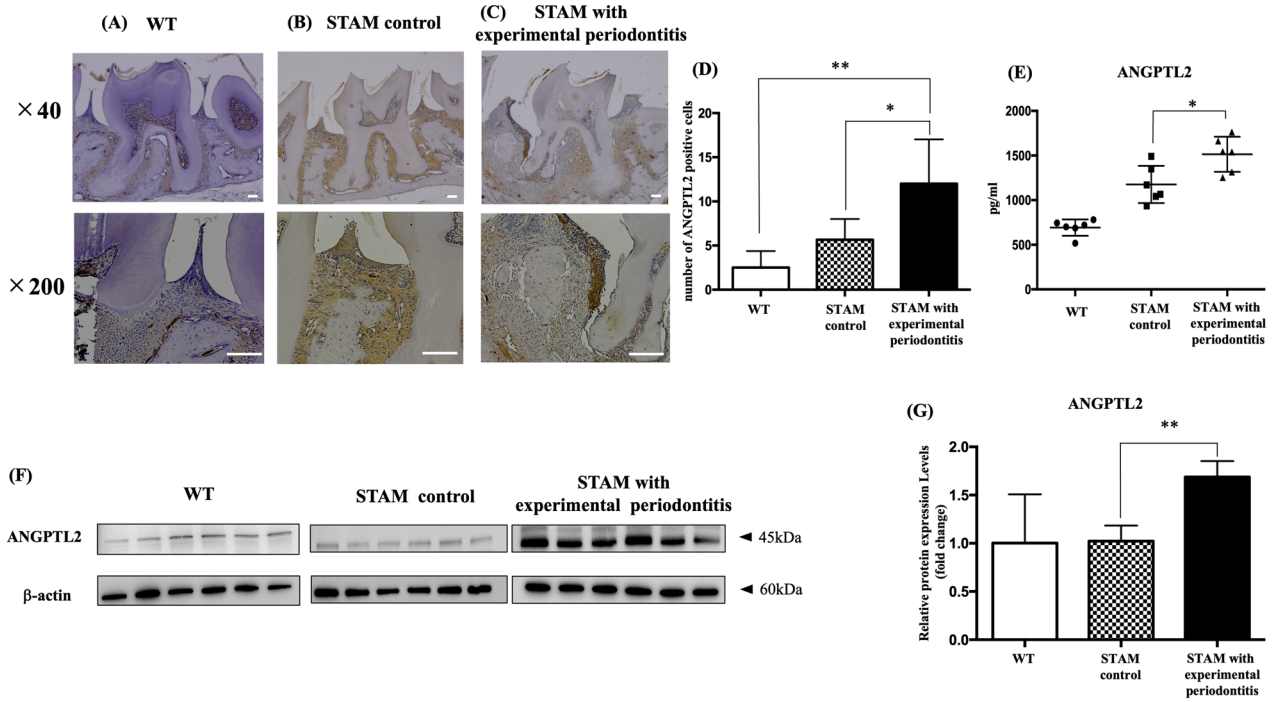

Figure 4. ANGPTL2 expression in STAM mice with experimental periodontitis. (**A**–**C**) ANGPTL2 protein in gingival tissue in 16-week-old STAM mice with experimental periodontitis is shown compared with that in wild-type mice and 16-week-old STAM mice without experimental periodontitis. Scale bar: 100 μm. (**D**) The numbers of ANGPTL2-positive cells per field (×200 magnification) are shown on the right side of each panel series. (**E**) ANGPTL2 levels were determined in the serum of STAM mice with or without experimental periodontitis using an ELISA kit. (**F**) The protein levels of ANGPTL2 and β-actin were detected in the livers of wild-type and STAM mice with or without experimental periodontitis using western blotting. Original blots/gels are presented in Appendix Fig. 3. (**G**) ANGPTL2 levels were measured by western blotting using Image J. Significant differences among groups were analyzed using one-way ANOVA and Tukey's test. Data are expressed as the mean ± SD ($n = 6$). $^{*}p < 0.05$, $^{**}p < 0.01$.

Administration of ANGPTL2 facilitates HCC growth in STAM mice

STAM mice intraperitoneally administered recombinant ANGPTL2 showed significant increases in the mean number of visible tumors larger than 2 mm and the mean maximum tumor diameter compared with 16-week-old STAM mice administered PBS (control) (Fig. 5A–D, J and K). However, the number of visible tumors was not significantly different between rANGPTL2-treated and control groups (Fig. 5I). H&E-stained sections showed that STAM mice administered rANGPTL2 exhibited more severe vacuolar degeneration in the liver than STAM mice administered PBS (Fig. 5E–H).

TNFα mRNA levels in the liver were significantly higher in STAM mice administered rANGPTL2 than in STAM mice administered PBS (Fig. 6A). mRNA levels of IL6, IL1β, Collagen 1, MMP9 and MMP2 tended to be higher in STAM mice administered rANGPTL2 than in STAM mice administered PBS (Fig. 6B–F). ANGPTL2 and ANGPTL4 mRNA levels were significantly higher in STAM mice administered rANGPTL2 than in STAM mice administered PBS (Fig. 6G, H).

Discussion

Here, we demonstrated the relationship between periodontitis and HCC in vivo for the first time using an animal model. Our results indicate that, as a result of periodontitis, ANGPTL2 is involved in HCC development.

Overexpression of ANGPTL2 accelerates HCC metastatic potential[13]. We demonstrated that the number of visible tumors over 2 mm was significantly greater in the periodontitis group than in the control group. In addition, gene expression of ANGPTL2, an inflammatory cytokine, and of MMPs was significantly increased in liver tissue of the periodontitis group. In fact, ANGPTL2 contributes to disease progression by promoting cancer migration and invasiveness through activation of transforming growth factor β1 (TGFβ) signaling, Rac signaling, and MMP expression[11].

Periodontitis increases ANGPTL2 expression and might enhance cancer progression. We previously reported that the ANGPTL2 levels in gingival crevicular fluid from chronic periodontitis patients were elevated, indicating that ANGPTL2 may regulate the inflammatory response in periodontitis[14]. We therefore assume that ANGPTL2 is a key mediator in periodontal disease and systemic diseases. Periodontal disease has been associated with several systemic diseases. For example, it is generally accepted that there is a bidirectional relationship between periodontal disease and diabetes. Gingival crevicular fluid and serum TNFα are inflammatory markers in patients with chronic periodontitis and type 2 diabetes[19]. Given that ANGPTL2 is homeostatic in the blood and acts systemically, we speculate that ANGPTL2 from periodontal tissue may not only be involved in periodontal tissue destruction, but may also act systemically[20]. In this study, ANGPTL2 production was elevated in periodontal tissue of STAM mice by ligature-induced periodontal inflammation. Additionally, ANGPTL2 protein abundance was elevated in peripheral blood in the periodontitis group. Furthermore, intraperitoneal administration of

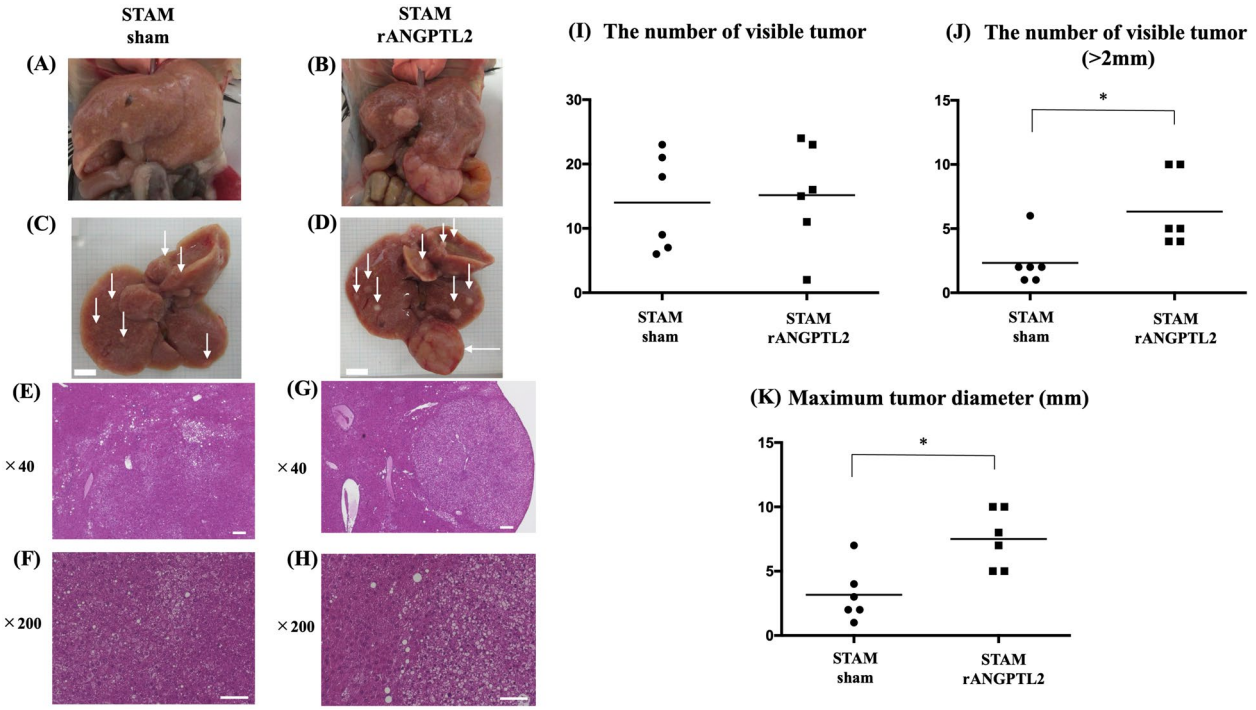

Figure 5. Macroscopic and histological features of STAM mice administered rANGPTL2. (**A**–**H**) Representative macroscopic appearance of the liver from STAM mice with or without intraperitoneal rANGPTL2 administration at 16 weeks. (**I**–**K**) Tumor characteristics of STAM mice with experimental periodontitis. Visible tumor counts are shown in (**I**). The number of visible tumors larger than 2 mm (**J**) and maximum tumor diameter (**K**) were determined. Significant differences among groups were analyzed using Tukey's test. Data are expressed as the mean ± SD ($n = 6$). *$p < 0.05$.

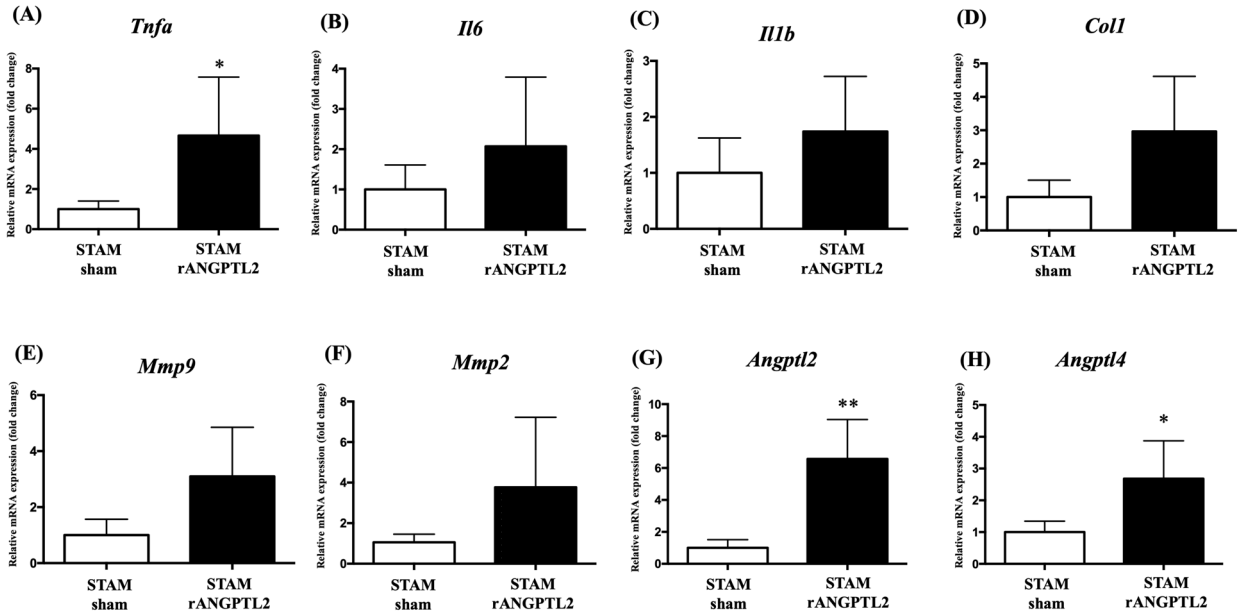

Figure 6. (**A**–**H**) Gene expression in the liver of STAM mice with or without rANGPTL2 administration at 16 weeks. mRNA levels of inflammatory cytokines (**A**–**C**), collagen type 1 (Col1) (**D**), MMP9 and 2 (**E**, **F**), and ANGPTL2 and 4 (**G**, **H**) were determined by quantitative real-time PCR. Significant differences among groups were analyzed using Tukey's test. Data are expressed as the mean ± SD ($n = 6$). $^{*}p < 0.05$, $^{**}p < 0.01$.

rANGPTL2 promoted HCC progression in STAM mice. These findings indicate that chronic inflammation and ANGPTL2 in periodontal tissue promote the pathogenesis of HCC via the bloodstream.

The oral cavity harbors the second most diverse microflora after the gut, which interacts with a variety of microorganisms in other parts of the body[21]. Oral dysbiosis is induced by periodontitis, and the bacteria associated with this might be swallowed[22]. Bacterial infection is a critical factor in triggering inflammation and alveolar bone resorption in the mouse ligature model used in this experiment[16]. Shi et al. reported that ligature-induced periodontitis in mice promoted colorectal cancer via alteration of microflora and suppression of immune reaction[23].

In chronic liver diseases, especially cirrhosis, swallowed oral bacteria may reach the intestine because of decreased gastric acid secretion[24]. The overgrowth of oral bacteria in the gut causes an inflammatory response that increases the permeability of the intestinal mucosa[25]. Microbe-associated molecular patterns, especially LPS, can then cross the damaged intestinal epithelial barrier and reach the liver via the portal circulation, inducing or exacerbating chronic hepatitis[22,25]. Meanwhile, many studies have supported the hypothesis that periodontopathogenic bacteria also directly cause liver damage[5,26–29]. Whether *P. gingivalis*, a typical bacterium associated with periodontal disease pathogenesis, plays a specific role in the etiology of HCC has not yet been evaluated; however, a role in another type of carcinogenesis has been reported[30]. *P. gingivalis* infection increased the number of lipid-containing hepatocytes and also resulted in increased levels of TNF and IL6 transcripts in the liver, which are strongly related to lipid droplet formation[27]. Fujita et al. tracked the biodistribution of radiolabeled *P. gingivalis* LPS from gingiva to liver and confirmed this endotoxin to be distributed in the liver[31]. Moreover, human HepG2 hepatocytes treated with oleic acid and LPS from *P. gingivalis* to mimic the NASH environment showed increased intracellular lipid accumulation and proinflammatory cytokines (IL1β and TNFα) compared with cells not treated with LPS[32]. Using a mouse model of periodontitis with ligatures, Mester et al. reported extensive vesicular lipidosis around the central hepatic vein and dilation of the portal vein caused by deposition of mature fibrous tissue[33]. IL6 and TNF activate NF-κB and STAT3, respectively, which are important for HCC development and progression[34]. We confirmed that expression of the TNFα gene was significantly increased in the experimental periodontitis and rANGPTL2 STAM mice groups. In contrast, IL1β and IL6 gene expression was not significantly increased in the experimental periodontitis and rANGPTL2 STAM mice groups. Giannoni et al. reported that cancer cells can secrete several types of growth factor, such as IL6 or TGFβ, which activate or stimulate cancer-associated fibroblasts and lead to their activation and the secretion of tumor-promoting growth factors[35]. In contrast, Fujii et al. reported no significant changes in IL6 gene expression in STAM mice, while TNFα gene expression was significantly increased, similar to our results[15]. MMP9 is a critical matrix proteinase that plays essential roles in malignancy progression[36]. In a study using a xenograft model with HCC and several HCC cell lines, it was found that circUBAP2, a novel circRNA whose expression is predominantly upregulated locally in HCC, promotes HCC progression via elevated MMP9[37]. MMP9 may contribute to the progression of HCC because its expression in liver is increased by the induction of periodontitis in STAM mice. Previous studies on the relationship between liver disease and periodontal disease have reported that oral periodontal pathogens might migrate to the liver and cause inflammation by elevating various mediators. Our findings indicate that ANGPTL2 might be a unique biomarker linking periodontal disease and HCC.

A positive correlation between periodontitis and overall cancer risk, including HCC, has been suggested epidemiologically[38]. In fact, HCC progression in patients with periodontitis was greater than that of HCC patients without periodontitis[7]. However, the detailed biological mechanism regarding the association between these two diseases has remained unknown. A schematic diagram illustrating the possible involvement of ANGPTL2 in periodontal disease and HCC is shown in Appendix Fig. 4. Our results support an immunological mechanism for the advance of liver disease by periodontitis and ANGPTL2. Future studies to fully understand the effects of periodontitis on liver disease (HCC) are warranted.

This study has several limitations. First, we were unable to directly identify factors involved in the progression of HCC due to periodontitis. The extent of their involvement needs to be clarified through studies using knockout mice of ANGPTL2, one of the candidate factors. Second, the effects of diabetes cannot be ruled out in the present experimental model because STAM mice have concomitant type 1 diabetes caused by streptozotocin-induced pancreatic destruction. Diabetes is an exacerbating factor for periodontitis, which may promote inflammation and accelerate HCC progression. The complexity of human NASH-HCC may not be fully mirrored in STAM model mice. Third, we consider the data insufficient to determine whether periodontitis primarily increases the incidence of HCC or the growth of HCC. This study did not analyze intracellular signaling pathways potentially leading to HCC progression. In future, in vitro studies and single-cell analyses should be performed to elucidate the mechanism of cancer progression. Fourth, we did not investigate polymicrobial synergy, or dysbiosis in the gut microbiota or oral microbiome. In future work, genetic analysis should be used to investigate the association with periodontal pathogens.

In conclusion, inflammation and bacteria in periodontal tissues might induce chronic inflammation in liver tissue via the bloodstream, resulting in HCC.

Data availability

The datasets generated during and/or analysed during the current study are available from the corresponding author on reasonable request.

Received: 24 February 2024; Accepted: 23 July 2024
Published online: 30 July 2024

References

1. Chaves, E. S., Jeffcoat, M. K., Ryerson, C. C. & Snyder, B. Persistent bacterial colonization of *Porphyromonas gingivalis*, *Prevotella intermedia*, and *Actinobacillus actinomycetemcomitans* in periodontitis and its association with alveolar bone loss after 6 months of therapy. *J. Clin. Periodontol.* **27**, 897–903. https://doi.org/10.1034/j.1600-051x.2000.027012897.x (2000).
2. Yamazaki, K. *et al.* Cytokine messenger RNA expression in chronic inflammatory periodontal disease. *Oral. Microbiol. Immunol.* **12**, 281–287. https://doi.org/10.1111/j.1399-302x.1997.tb00392.x (1997).
3. Preshaw, P. M. *et al.* Periodontitis and diabetes: A two-way relationship. *Diabetologia* **55**, 21–31. https://doi.org/10.1007/s00125-011-2342-y (2012).
4. Ishikawa, M. *et al.* Oral *Porphyromonas gingivalis* translocates to the liver and regulates hepatic glycogen synthesis through the Akt/GSK-3beta signaling pathway. *Biochim Biophys. Acta* **1832**, 2035–2043. https://doi.org/10.1016/j.bbadis.2013.07.012 (2013).
5. Furusho, H. *et al.* Dental infection of *Porphyromonas gingivalis* exacerbates high fat diet-induced steatohepatitis in mice. *J. Gastroenterol.* **48**, 1259–1270. https://doi.org/10.1007/s00535-012-0738-1 (2013).
6. Matsuda, Y. *et al.* Ligature-induced periodontitis in mice induces elevated levels of circulating interleukin-6 but shows only weak effects on adipose and liver tissues. *J. Periodontal. Res.* **51**, 639–646. https://doi.org/10.1111/jre.12344 (2016).
7. Tamaki, N. *et al.* Stage of hepatocellular carcinoma is associated with periodontitis. *J. Clin. Periodontol.* **38**, 1015–1020. https://doi.org/10.1111/j.1600-051X.2011.01777.x (2011).
8. Vogel, A., Meyer, T., Sapisochin, G., Salem, R. & Saborowski, A. Hepatocellular carcinoma. *Lancet* **400**, 1345–1362. https://doi.org/10.1016/S0140-6736(22)01200-4 (2022).
9. Santulli, G. Angiopoietin-like proteins: a comprehensive look. *Front. Endocrinol.* **5**, 4. https://doi.org/10.3389/fendo.2014.00004 (2014).
10. Kim, I. *et al.* Molecular cloning, expression, and characterization of angiopoietin-related protein. angiopoietin-related protein induces endothelial cell sprouting. *J. Biol. Chem.* **274**, 26523–26528. https://doi.org/10.1074/jbc.274.37.26523 (1999).
11. Endo, M. *et al.* Tumor cell-derived angiopoietin-like protein ANGPTL2 is a critical driver of metastasis. *Cancer Res.* **72**, 1784–1794. https://doi.org/10.1158/0008-5472.CAN-11-3878 (2012).
12. Tian, Z. *et al.* Perivascular adipose tissue-secreted angiopoietin-like protein 2 (Angptl2) accelerates neointimal hyperplasia after endovascular injury. *J. Mol. Cell Cardiol.* **57**, 1–12. https://doi.org/10.1016/j.yjmcc.2013.01.004 (2013).
13. Gao, L. *et al.* ANGPTL2 promotes tumor metastasis in hepatocellular carcinoma. *J. Gastroenterol. Hepatol.* **30**, 396–404. https://doi.org/10.1111/jgh.12702 (2015).
14. Ohno, T. *et al.* Angiopoietin-like protein 2 regulates *Porphyromonas gingivalis* lipopolysaccharide-induced inflammatory response in human gingival epithelial cells. *PLoS ONE* **12**, e0184825. https://doi.org/10.1371/journal.pone.0184825 (2017).
15. Fujii, M. *et al.* A murine model for non-alcoholic steatohepatitis showing evidence of association between diabetes and hepatocellular carcinoma. *Med. Mol. Morphol.* **46**, 141–152. https://doi.org/10.1007/s00795-013-0016-1 (2013).
16. Abe, T. & Hajishengallis, G. Optimization of the ligature-induced periodontitis model in mice. *J. Immunol. Methods* **394**, 49–54. https://doi.org/10.1016/j.jim.2013.05.002 (2013).
17. Faul, F., Erdfelder, E., Lang, A. G. & Buchner, A. G*Power 3: a flexible statistical power analysis program for the social, behavioral, and biomedical sciences. *Behav. Res. Methods* **39**, 175–191. https://doi.org/10.3758/bf03193146 (2007).
18. Goto, H. *et al.* Ebi3 knockout aggravates experimental periodontitis via Th17 polarization. *J. Clin. Periodontol.* **50**, 1406–1418. https://doi.org/10.1111/jcpe.13859 (2023).
19. Singhal, S., Pradeep, A. R., Kanoriya, D. & Garg, V. Human soluble receptor for advanced glycation end products and tumor necrosis factor-alpha as gingival crevicular fluid and serum markers of inflammation in chronic periodontitis and type 2 diabetes. *J. Oral Sci.* **58**, 547–553. https://doi.org/10.2334/josnusd.16-0017 (2016).
20. Tabata, M. *et al.* Angiopoietin-like protein 2 promotes chronic adipose tissue inflammation and obesity-related systemic insulin resistance. *Cell Metab.* **10**, 178–188. https://doi.org/10.1016/j.cmet.2009.08.003 (2009).
21. Kitamoto, S., Nagao-Kitamoto, H., Hein, R., Schmidt, T. M. & Kamada, N. The bacterial connection between the oral cavity and the gut diseases. *J. Dent. Res.* **99**, 1021–1029. https://doi.org/10.1177/0022034520924633 (2020).

22. Albuquerque-Souza, E. & Sahingur, S. E. Periodontitis, chronic liver diseases, and the emerging oral-gut-liver axis. *Periodontol* **2000**(89), 125–141. https://doi.org/10.1111/prd.12427 (2022).
23. Shi, Y. T. *et al.* Ligature-induced periodontitis drives colorectal cancer: An experimental model in mice. *J. Dent. Res.* **102**, 689–698. https://doi.org/10.1177/00220345231158269 (2023).
24. Qin, N. *et al.* Alterations of the human gut microbiome in liver cirrhosis. *Nature* **513**, 59–64. https://doi.org/10.1038/nature13568 (2014).
25. Kapil, S. *et al.* Small intestinal bacterial overgrowth and toll-like receptor signaling in patients with non-alcoholic fatty liver disease. *J. Gastroenterol. Hepatol.* **31**, 213–221. https://doi.org/10.1111/jgh.13058 (2016).
26. Nakahara, T. *et al.* Involvement of *Porphyromonas gingivalis* in the progression of non-alcoholic fatty liver disease. *J. Gastroenterol.* **53**, 269–280. https://doi.org/10.1007/s00535-017-1368-4 (2018).
27. Arimatsu, K. *et al.* Oral pathobiont induces systemic inflammation and metabolic changes associated with alteration of gut microbiota. *Sci. Rep.* **4**, 4828. https://doi.org/10.1038/srep04828 (2014).
28. Nagasaki, A. *et al.* Odontogenic infection by *Porphyromonas gingivalis* exacerbates fibrosis in NASH via hepatic stellate cell activation. *Sci. Rep.* **10**, 4134. https://doi.org/10.1038/s41598-020-60904-8 (2020).
29. Varela-Lopez, A. *et al.* A diet rich in saturated fat and cholesterol aggravates the effect of bacterial lipopolysaccharide on alveolar bone loss in a rabbit model of periodontal disease. *Nutrients* https://doi.org/10.3390/nu12051405 (2020).
30. Olsen, I. & Yilmaz, O. Possible role of *Porphyromonas gingivalis* in orodigestive cancers. *J. Oral. Microbiol.* **11**, 1563410. https://doi.org/10.1080/20002297.2018.1563410 (2019).
31. Fujita, M. *et al.* Histological effects and pharmacokinetics of lipopolysaccharide derived from *Porphyromonas gingivalis* on rat maxilla and liver concerning with progression into non-alcoholic steatohepatitis. *J. Periodontol.* **89**, 1101–1111. https://doi.org/10.1002/JPER.17-0678 (2018).
32. Ding, L. Y. *et al. Porphyromonas gingivalis*-derived lipopolysaccharide causes excessive hepatic lipid accumulation via activating NF-kappaB and JNK signaling pathways. *Oral Dis.* **25**, 1789–1797. https://doi.org/10.1111/odi.13153 (2019).
33. Mester, A. *et al.* Periodontal disease may induce liver fibrosis in an experimental study on Wistar rats. *J. Periodontol.* **90**, 911–919. https://doi.org/10.1002/JPER.18-0585 (2019).
34. Naugler, W. E. *et al.* Gender disparity in liver cancer due to sex differences in MyD88-dependent IL-6 production. *Science* **317**, 121–124. https://doi.org/10.1126/science.1140485 (2007).
35. Giannoni, E. *et al.* Reciprocal activation of prostate cancer cells and cancer-associated fibroblasts stimulates epithelial-mesenchymal transition and cancer stemness. *Cancer Res.* **70**, 6945–6956. https://doi.org/10.1158/0008-5472.CAN-10-0785 (2010).
36. Lu, L. *et al.* Hepatitis C virus NS3 protein enhances cancer cell invasion by activating matrix metalloproteinase-9 and cyclooxygenase-2 through ERK/p38/NF-kappaB signal cascade. *Cancer Lett.* **356**, 470–478. https://doi.org/10.1016/j.canlet.2014.09.027 (2015).
37. Liu, B. *et al.* CircUBAP2 promotes MMP9-mediated oncogenic effect via sponging miR-194-3p in hepatocellular carcinoma. *Front. Cell Dev. Biol.* **9**, 675043. https://doi.org/10.3389/fcell.2021.675043 (2021).
38. Michaud, D. S., Fu, Z., Shi, J. & Chung, M. Periodontal disease, tooth loss, and cancer risk. *Epidemiol. Rev.* **39**, 49–58. https://doi.org/10.1093/epirev/mxx006 (2017).

Acknowledgements
We thank Edanz (https://jp.edanz.com/ac) for proofreading a draft of this manuscript.

Author contributions
T.O., T.K., J.H., E.N., G.Y., S.N., A.M. contributed to conception and design. T.O., Y.S., R.G., D.T., S.K., K.O. contributed to data acquisition and analysis. T.O., T.K., S.N., A.M. contributed to data interpretation. T.O., T.K., Y.S., R.G., R.G., D.T., S.K., K.O. drafted the manuscript. T.K., J.H., E.N., G.Y., S.N., A.M. critically revised the manuscript. All authors gave their final approval and agree to be accountable for all aspects of the work.

Funding
This work was supported by a Grant-in-Aid for Young Scientists (grant no. 20K18519) from the Ministry of Education, Culture, Sports, Science and Technology (Tokyo, Japan) and the Orange Fund for the Commemoration of Hokkaido Hepatitis B Lawsuits (2021 to 2023).

Competing interests
The authors declare no competing interests.

Additional information
Supplementary Information The online version contains supplementary material available at https://doi.org/10.1038/s41598-024-68422-7.

Correspondence and requests for materials should be addressed to T.K.